Physics Letters B 807 (2020) 135527

Contents lists available at ScienceDirect

Physics Letters B

www.elsevier.com/locate/physletb

Fifth-force search with the bound-electron g factor

V. Debierre, C.H. Keitel, Z. Harman

Max Planck Institute for Nuclear Physics, Saupfercheckweg 1, 69117 Heidelberg, Germany

ARTICLE INFO

Article history:
Received 17 February 2020
Received in revised form 22 May 2020
Accepted 28 May 2020
Available online 1 June 2020
Editor: A. Ringwald

ABSTRACT

The use of high-precision measurements of the g factor of few-electron ions and its isotope shifts is put forward as a probe for physics beyond the Standard Model. The contribution of a hypothetical fifth fundamental force to the g factor is calculated for the ground state of H-like, Li-like and B-like ions, and employed to derive bounds on the parameters of that force. The weighted difference and especially the isotope shift of g factors are used in order to increase the experimental sensitivity to the new physics contribution. It is found that, combining measurements from four different isotopes of H-like, Li-like and B-like calcium ions at accuracy levels projected to be accessible in the near future, experimental results compatible with King planarity would constrain the new physics coupling constant more than one order of magnitude further than the best current atomic data and theory.

1. Introduction

The g factors of the free electron and free muon have served as precision tests for quantum electrodynamics (QED), the Standard Model (SM) more broadly, and possible extensions of the SM [1–7]. In parallel, recent years have seen rapid improvements in the experimental [8–12] and theoretical [13–21] determination of the g factor of bound electrons (for a review, see Ref. [22]), owing to the accelerating development of bound-state quantum field theory [13–21,23–26]. This allows for stringent tests of QED in strong fields, and, to a lesser extent, other sectors of the SM, and can hence be a route for the discovery of phenomena beyond the SM. In the present work, we demonstrate the effectiveness of the g factor of bound electrons in the search for new physics (NP).

A relatively direct method consists in comparing the best available theoretical and experimental results. The largest difference between these results allowed by the uncertainties, provides a bound for the NP contribution to the g factor. With this method, we also use data on weighted differences of g factors of ions in different charge states [27–30].

Another method is centered on the isotope shift. Precision spectroscopy of the isotope shifts in optical transition frequencies in ions has recently been used [31–34] to examine hypothetical new fundamental forces. When specific candidates for forces are considered, this examination of the isotope shift provides a more direct route to test NP than do high-precision QED calculations. In this work, we generalize this method to g-factor precision spectroscopy. Considering four different isotopes of a given ion and two different electronic states, a specific feature in the yet-to-be-obtained g-factor isotope-shift data, known as King nonplanarity, could be, with some care, understood as a potential signature of NP. For this conclusion to be warranted, it would need to be assumed that the hypothetical force considered here dominates over other beyond-SM contributions. Conversely, a lack of King nonplanarity in the data would allow the setting of competitive bounds on NP. In order to obtain bounds on the NP parameters, we first derive the correction to the bound-electron g factor due to a hypothetical fifth force.

2. Correction to the g factor due to a massive scalar boson

New scalar bosons have been proposed as a solution to the long-standing electroweak hierarchy problem [35]. These massive scalar bosons would mediate a fifth force, resulting in an interaction between nucleons and electrons, by coupling to both particle types in a spin-independent way [31,32,34]. The potential exerted on electrons by this hypothetical force is of the Yukawa type [33]:

$$V_\phi(\mathbf{r}) = -\hbar c\,\alpha_{\mathrm{NP}}\,A\,\frac{\mathrm{e}^{-\frac{m_\phi c}{\hbar}|\mathbf{r}|}}{|\mathbf{r}|}, \tag{1}$$

where m_ϕ is the mass of the boson, $\alpha_{\mathrm{NP}} = y_e y_n/4\pi$ is the new-physics coupling constant, with y_e and y_n the coupling of the massive scalar boson to the electrons and the nucleons, respectively, $\hbar$ and c are Planck's reduced constant and the vacuum

E-mail addresses: vincent.debierre@mpi-hd.mpg.de (V. Debierre), zoltan.harman@mpi-hd.mpg.de (Z. Harman).

https://doi.org/10.1016/j.physletb.2020.135527

Fig. 1. Feynman diagram corresponding to the hypothetical NP contribution to the g factor of a bound electron. The double line represents the bound electron, the wavy line terminated by a triangle denotes a photon from the external magnetic field, and the dashed line terminated by a square denotes a scalar boson from the nucleons.

velocity of light, and A is the number of nucleons in the considered nucleus. For completeness, we treat the ions of interest in a fully relativistic manner, also noting interesting investigations in the non-relativistic limit [36,37].

The first-order correction to the g factor of a bound electron in the quantum state a due to this potential is given by the diagram in Fig. 1, together with the one in which the order of the two interactions is swapped. Together they yield

$$\Delta g_a = -2\alpha_{\mathrm{NP}}\, A\, \frac{\hbar c}{\mu_0 B m_a} \int_0^{+\infty} \mathrm{d}r\, r\, \mathrm{e}^{-\frac{m_\phi c}{\hbar} r} \times \left[g_a(r)\, X_a(r) + f_a(r)\, Y_a(r) \right], \quad (2)$$

where $\mu_0 = e\hbar/2m_e$ is the Bohr magneton, m_a the magnetic quantum number of state a, B the magnitude of the external, static, homogeneous magnetic field, and X_a and Y_a the corrections to the large (g_a) and small (f_a) components of the bound electron radial wave function, due to the interaction with the magnetic field, given in Ref. [38]. For the H-like ground state $a = 1s$, we obtain

$$\Delta g_{1s} = -\frac{4}{3}\alpha_{\mathrm{NP}} \frac{(Z\alpha)}{\gamma} A \left(1 + \frac{m_\phi}{2Z\alpha m_e}\right)^{-2\gamma} \times \left[3 - 2\frac{(Z\alpha)^2}{1+\gamma} - \frac{2\gamma}{1 + \frac{m_\phi}{2Z\alpha m_e}}\right] \quad (3)$$

where $\gamma = \sqrt{\kappa^2 - (Z\alpha)^2}$ with κ the relativistic angular quantum number and Z the number of protons. The full exact results for the $a = 2s$ ground state of Li-like ions, and for the $a = 2p_{1/2}$ ground state of B-like ions, are given in the Supplemental Material. However, common asymptotics for all s states can be given for simplicity in the nonrelativistic limit: in the intermediate mass regime $Z\alpha m_e \ll m_\phi \ll \hbar/r_N c$ (r_N is the nuclear radius), we derive

$$\Delta g_{ns}^{\mathrm{nonrel}} \simeq -\frac{16}{3}\alpha_{\mathrm{NP}}\, A\, \frac{Z\alpha}{n^3} \left(Z\alpha \frac{m_e}{m_\phi}\right)^2 \left[3 - 16\, Z\alpha\, \frac{m_e}{m_\phi}\right], \quad (4a)$$

while in the small mass regime $m_\phi \ll Z\alpha m_e$, we obtain

$$\Delta g_{ns}^{\mathrm{nonrel}} \simeq -\frac{4}{3}\alpha_{\mathrm{NP}}\, A\, \frac{Z\alpha}{n^2} \quad (4b)$$

Here n is the principal quantum number of the s state considered. With the help of our exact results (that is, Eq. (3) and the corresponding results for $2s$ and $2p_{1/2}$), we will set bounds on NP in what follows. The free parameters to be constrained are the coupling constant α_{NP} and the boson mass m_ϕ. Existing constraints coming from various areas of physics (Casimir force measurements, globular cluster data and neutron scattering experiments) are given by the solid blue curves in Fig. 2. Bounds from supernova data [39,40] are too strong to appear on the corresponding plot, but the reader can consult Refs. [31,33].

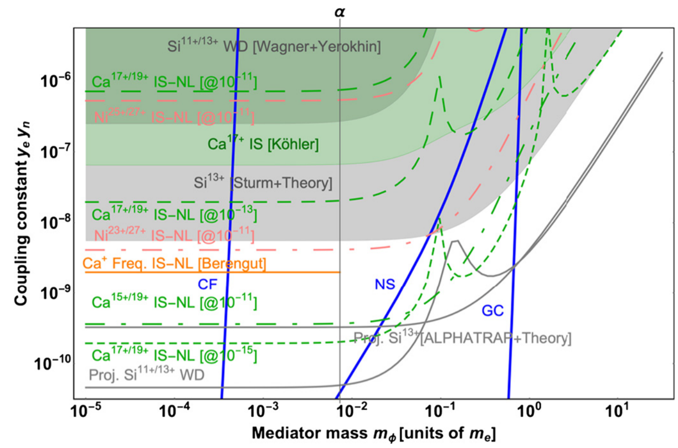

Fig. 2. Bounds on the New Physics coupling constant $y_e y_n = 4\pi\alpha_{\mathrm{NP}}$ as a function of the scalar boson mass m_ϕ. The regions above and to the left of the solid blue curves are excluded by Casimir force (CF) measurements [45], globular cluster (GC) data [46], and neutron scattering (NS) experiments [47]. The shaded regions are excluded by available g-factor data, and the regions above the curves are excluded by projected g-factor data. The thick orange line refers to the small-mass limit of the bound obtained in Ref. [31] from isotope shift measurements in transition frequencies in Ca^+. Two regions refer to available data on silicon (gray: $^{28}\mathrm{Si}^{13+}$ ([Sturm+Theory]) [9], dark green: $^{28}\mathrm{Si}^{11/13+}$ ([Wagner+Yerokhin]) [29,30]). The solid gray curves refer to projected bounds for silicon (upper: $^{28}\mathrm{Si}^{13+}$ [9], lower: $^{28}\mathrm{Si}^{11/13+}$ [29,30]), provided the calculation of radiative corrections is advanced and theory becomes limited by nuclear radius uncertainties. The light green region refers to the calcium isotope shift ($^{40/48}\mathrm{Ca}^{17+}$ ([Köhler]) [48]). All other curves represent projected bounds from a King analysis of the g factor (IS-NL: Isotope Shift-Nonlinearity). The green curves refer to projected bounds for calcium [sparsely dashed (resp. dashed, densely dashed): projections on $^{40/42/44/48}\mathrm{Ca}^{17+/19+}$ assuming King planarity (KP) at the relative experimental accuracy of 10^{-11} (resp. 10^{-13}, 10^{-15}), dot-dashed: projections on $^{40/42/44/48}\mathrm{Ca}^{15+/19+}$ (KP at 10^{-11})]. The pink curves refer to nickel [dashed: projections on $^{58/60/62/64}\mathrm{Ni}^{25+/27+}$ (KP at 10^{-11}), dot-dashed: projections on $^{58/60/62/64}\mathrm{Ni}^{23+/27+}$ (KP at 10^{-11})].

3. Tests with g factors and their weighted difference

A first set of bounds can be obtained straightforwardly, by considering that the NP contribution to the g factor is bounded by current uncertainties on the g factor. Let us consider the case of H-like $^{28}\mathrm{Si}^{13+}$. Using Eq. (3) and the difference $\Delta g \simeq 1.7 \times 10^{-9}$ [10,20] between theory and experiment (we take the maximum difference allowed by the uncertainties, making use of the updated electron mass uncertainty [11]), we exclude the larger gray region ([Sturm+Theory]) in Fig. 2. The current theoretical uncertainties are 3×10^{-11} from the finite nuclear size correction [41], and 6×10^{-10} from QED radiative corrections [20], meaning that improvement of the QED theory would be meaningful up to a factor of 20, yielding the bound represented by the upper solid gray curve (Proj. Si^{13+}) in Fig. 2 if the agreement with experiments remains at that level of precision.

As this example illustrates, the finite nuclear size correction is a major source of uncertainty in the calculation of bound-electron g factors. To circumvent this, it has been proposed to use weighted differences of g factors of electrons in the $1s$ and $2s$ states [27,29,30], as well as in the $1s$ and $2p_{1/2}$ states [28]. These are given [28–30,42,43] by

$$\delta_{\xi_s} g = g_{2s} - \xi_s g_{1s}, \quad \delta_{\xi_p} g = g_{2p_{1/2}} - \xi_p g_{1s}, \quad (5a)$$

$$\xi_s = 2^{-(1+2\gamma)}\left[1 + \frac{3}{16}(Z\alpha)^2\right], \quad (5b)$$

$$\xi_p = 2^{-(5+2\gamma)}\, 3\, (Z\alpha)^2 \left[1 + \frac{35}{256}(Z\alpha)^2\right]. \quad (5c)$$

In the weighted difference, the finite nuclear size corrections almost entirely cancel each other, through a careful choice of the ξ

coefficients. Using the combined experimental and theoretical data on the $1s$–$2s$ weighted difference in $^{28}\mathrm{Si}^{13+}$ from Refs. [29,30], we exclude the dark green area ([Wagner+Yerokhin]) in Fig. 2. Here, QED theory can be improved [29,44] up to a factor of 10^4 (yielding the bound represented by the lower solid gray curve (Proj. $\mathrm{Si}^{11+/13+}$ WD) if the agreement with experiments remains at that level of precision) before the theoretical uncertainty becomes dominated by the finite nuclear size correction. This represents a promising avenue for the setting of more stringent bounds on NP. We note that, in principle, subtleties arise in the derivation of bounds in the limit of low scalar boson masses [37], due to the fact that, in this limit, the Yukawa potential (1) becomes indistinguishable from a Coulomb potential, which causes an effective correction $\alpha \to \alpha + \alpha_{\mathrm{NP}}$ to the fine-structure constant. A method to disentangle a possible nonzero α_{NP} with the uncertainties of α is presented in detail in Ref. [37]. For our purposes, measurements of the bound-electron g factor can be combined with measurements of the free-electron g factor, the most precise of which was reported in Ref. [2], and was at the time providing the most precise determination of α. Since the free-electron g factor is not sensitive to the type of NP considered in the present work, and since it has been measured [2] with a relative uncertainty two orders of magnitude smaller than the best measurements of the bound-electron g factor [10], the bounds which we derived are only affected by this subtlety at the level of 1% or smaller, as can be seen from Eqs. (3.19) and (3.26) of Ref. [37].

4. Isotope shifts and the King representation

We now turn to the analysis of isotope shifts. Consider two states 1 and 2 of a bound electron in an ion. For both states, considering two isotopes A and A' of the same ion, we write [49] the isotope shift in the g factor as

$$g_i^{AA'} = g_i^A - g_i^{A'}\,, \quad i \in \{1,2\}\,. \tag{6}$$

There has already been experimental [48] and theoretical [50] interest in g-factor isotope shifts. We emphasize that experimental data could soon be collected with a relative precision going up to 11 digits for the isotope shift [51]. In the SM, the isotope shift is given at the leading order in the electron-to-nucleus mass ratios $m_e/M_{A^{(\prime)}}$ and the nuclear radii $\langle r^2\rangle_{A^{(\prime)}}$ by

$$g_{i(\mathrm{SM})}^{AA'} = K_i\,\mu_{AA'} + F_i\,\delta\left\langle r^2\right\rangle_{AA'}, \tag{7}$$

where $\mu_{AA'} = 1/M_A - 1/M_{A'}$. The first summand on the r.h.s. is the mass shift, originating from the difference between the masses M_A and $M_{A'}$ of the two isotopes. The second summand is the field shift, and originates from the difference $\delta\langle r^2\rangle_{AA'} = \langle r^2\rangle_A - \langle r^2\rangle_{A'}$ in the nuclear charge radii between the two isotopes. The only quantities that depend on the specific electronic level considered are explicitly referred to as such by the label i. Notice that radiative QED corrections to the g factor are largely absent from the isotope shift, as they are approximately the same for all isotopes of a given ion. Taking account of the hypothetical NP contribution (2) to the g factor, the isotope shift becomes (in analogy to Refs. [31,32])

$$g_{i(\mathrm{NP})}^{AA'} = K_i\,\mu_{AA'} + F_i\,\delta\left\langle r^2\right\rangle_{AA'} + \alpha_{\mathrm{NP}} X_i \gamma_{AA'}. \tag{8}$$

As can be seen from Eq. (2), $\gamma_{AA'} = A - A'$. The parameters of the hypothetical fifth force can be constrained through a study of the isotope shift in the g factor. Indeed, the presence of the third contribution to the isotope shift in Eq. (8) can be detected on King plots. Let us introduce $G_i^{AA'} \equiv g_i^{AA'}/\mu_{AA'}$ as well as $h_{AA'} \equiv \gamma_{AA'}/\mu_{AA'}$. The King representation is now constructed from considering four different isotopes A, A'_1, A'_2, A'_3. We introduce the notations

$$\mathbf{G}_i \equiv \left(G_i^{AA'_1}, G_i^{AA'_2}, G_i^{AA'_3}\right), \tag{9a}$$

$$\mathbf{h} \equiv \left(h^{AA'_1}, h^{AA'_2}, h^{AA'_3}\right), \qquad \mathbf{A}_{\mathrm{tt}} \equiv (1,1,1)\,. \tag{9b}$$

King nonplanarity is measured [31] by the parameter

$$\mathcal{N} \equiv \frac{1}{2}\left(\mathbf{G}_1 \times \mathbf{G}_2\right)\cdot \mathbf{A}_{\mathrm{tt}} \tag{10}$$

and, while, in the SM, it is easily seen that $\mathcal{N}_{\mathrm{SM}} = 0$ at the leading order, in the presence of NP, the nonplanarity reads

$$\mathcal{N}_{\mathrm{NP}} = \frac{\alpha_{\mathrm{NP}}}{2}\left(\mathbf{A}_{\mathrm{tt}} \times \mathbf{h}\right)\cdot\left(X_1 \mathbf{G}_{2(\mathrm{NP})} - X_2 \mathbf{G}_{1(\mathrm{NP})}\right). \tag{11}$$

Hence nonplanarity in the King representation is a possible sign of NP. However, other corrections cause departures from planarity. Indeed the SM contributions (7) to the isotope shift are only valid at the leading order. Subleading (nuclear) SM contributions to the isotope shift are another source of nonplanarity. As such, one should be careful before interpreting potential observed nonplanarities as a sign of NP.

5. Standard model contributions to King nonplanarity

Several subleading nuclear corrections to the g factor induce King nonplanarity in the SM, which limits the range of nonplanarity as a signature of NP to an extent that can be quantified (see Supplemental Material, also see Ref. [52] where subleading nuclear corrections are calculated for the transition frequencies of argon ions). These corrections are a higher-order contribution to the finite nuclear size correction [53], the nuclear polarization correction [54,55], the nuclear deformation correction [56,57], which all contribute to the field shift, and the higher-order mass correction [58]. We have evaluated these contributions using Eq. (15) of Ref. [53], Eq. (26) of Ref. [32],[1] Eqs. (8)–(12) of Ref. [56], and Eq. (47) of Ref. [58]. We take the nuclear charge radius values found in Ref. [61] and the nuclear deformation parameters found in Ref. [62]. The higher-order finite nuclear size correction is not given in the literature for p states: we built an upper bound for $2p_{1/2}$ by considering that it scales, with respect to the leading-order, in the same way that it does for $2s$, with an extra factor of 10. In the Supplemental Material, we indicate the various contributions to the King nonplanarity from these subleading nuclear corrections, for a few cases that are considered in this work. We do not consider radiative corrections to the leading nuclear recoil and finite size contributions here. The radiative recoil correction brings a small correction to the coefficient K_i, and hence no King nonplanarities. The radiative size correction brings a small contribution to the coefficient F_i, plus a small contribution [63] that is one order of magnitude smaller than the four subleading nuclear corrections considered here, and which can hence safely be neglected. All radiative corrections to the coefficients K_i and F_i mentioned just above are less than a few percent relative to the value of K_i and F_i, and hence do not appreciably change the derived bounds.

[1] The evaluation of the nuclear polarization correction to the g factor according to Eq. (26) of Ref. [32] yields results which tend to overevaluate the more precisely calculated correction [54] by a factor of ~ 2, but, in the case of transition energies, it tends to underevaluate the isotope shift itself by a factor of ~ 2, as can be checked by comparison with the results reported in Ref. [59] (which should be divided by (2π) [60]). We have checked that artificially multiplying the results for the nuclear polarization correction to the g factor obtained through the method of Ref. [32] by a factor of 2 does not appreciably change the obtained bounds on NP. A more complete treatment of this correction could be relevant for future investigations.

6. Tests with the isotope shift

A first set of bounds on NP can be obtained by considering simple isotope shifts, without recourse to the King formalism. The shift in the g factor between the $^{40}Ca^{17+}$ and $^{48}Ca^{17+}$ isotopes of Li-like calcium [48,50] has been calculated to be $\Delta g_{\mathrm{th}} = 11.056\,(16) \times 10^{-9}$ in the SM, while the experimental value is $\Delta g_{\mathrm{xp}} = 11.70\,(1.39) \times 10^{-9}$, meaning that the error bars allow for a maximum difference of $\Delta g \simeq 2.05 \times 10^{-9}$. With the NP correction (2) to the g factor in the $2s$ state, this leads to the exclusion of the light green region ([Köhler]) in Fig. 2.

Bounds on NP from King planarity tests are obtained in the following way: the nonplanarity parameter (10) computed from (in our case, simulated) experimental data is first compared to its first-order propagated error $\sigma_{\mathcal{N}}$, as explained in Ref. [31]. If $\mathcal{N} < \sigma_{\mathcal{N}}$, the data is considered planar, and we use the first-order propagated error $\sigma_{\alpha_{\mathrm{NP}}}$ as the upper bound for α_{NP}. To compute $\sigma_{\alpha_{\mathrm{NP}}}$, we have generalized Eq. (8), taking account of the subleading nuclear corrections to the g factor that induce King nonplanarity in the SM:

$$g_{i(\mathrm{TN})}^{AA'} = K_i\, \mu_{AA'} + F_i\, \delta \left\langle r^2 \right\rangle_{AA'} + \alpha_{\mathrm{NP}} X_i \gamma_{AA'} + s_{i\,AA'}. \tag{12}$$

Here the subscript (TN) indicates that the total King nonplanarity is captured, including its SM contributions. Note that $s_{i\,AA'}$, the contribution to the isotope shift from these subleading nuclear corrections, cannot be factorized as the product of a nuclear term and an electronic term. Setting $S_{i\,AA'} \equiv s_{i\,AA'}/\mu_{AA'}$ and

$$\mathbf{S}_i \equiv \left(S_i^{AA'_1}, S_i^{AA'_2}, S_i^{AA'_3} \right), \tag{13}$$

we obtain

$$\mathcal{N}_{\mathrm{TN}} = -\frac{\mathbf{A}_{\mathrm{tt}}}{2} \cdot \left[\mathbf{G}_{1(\mathrm{TN})} \times \left(\frac{F_2}{F_1} \mathbf{S}_1 - \mathbf{S}_2 \right) - (1 \leftrightarrow 2) \right] + \frac{\alpha_{\mathrm{NP}}}{2} \left(\mathbf{A}_{\mathrm{tt}} \times \mathbf{h} \right) \cdot \left[\left(X_1 \frac{F_2}{F_1} - X_2 \right) \mathbf{G}_{1(\mathrm{TN})} - (1 \leftrightarrow 2) \right] \tag{14}$$

which can be checked to simplify to its equivalent Eq. (11) in the $\mathbf{S}_i \to \mathbf{0}$ limit, where the subleading nuclear corrections are neglected. It is then straightforward from Eq. (14), to compute α_{NP} and its propagated error $\sigma_{\alpha_{\mathrm{NP}}}$. The leading-order mass and field shifts in Eq. (7) are computed according to Refs. [42,50,64,65].

We thus derive bounds from possible future experiments on the spinless $A = 40$, 42, 44, 48 isotopes of calcium. We first use the $1s$ and $2s$ states (the respective ground state of the H-like and Li-like ions), for the explicit realization of our analysis. Assuming that the experimental data for the H-like and Li-like ground states will be compatible with King planarity, and that the relative experimental uncertainties on the measured g factors will be 10^{-11}, 10^{-13} and 10^{-15}, respectively,[2] we obtain the projected bounds given by the three dashed green curves in Fig. 2. This assumes that the mass uncertainty of the Ca ions will be reduced by up to two orders of magnitude, which can be achieved by the newly commissioned PENTATRAP Penning-trap setup [51,66–68]. We also consider the $A = 58$, 60, 62, 64 isotopes of nickel.[3] With the same reasoning, and with hypothetical data with the uncertainty 10^{-11}, we obtain

[2] We recall that such precise results can be obtained by a direct measurement of the g-factor isotope shift [51].

[3] The choice of the atomic elements is motivated by the existence of four spinless isotopes. It is also motivated by the fact that calcium and nickel possess a magic nucleus, and, in the case of ^{40}Ca and ^{48}Ca, a double magic nucleus. The nuclear deformation and polarization corrections are unusually small for magic nuclei, suppressing the SM contribution to King nonplanarity, which is favorable for our purposes. Further motivation is provided by the easy availability of highly charged calcium ions for g-factor measurements.

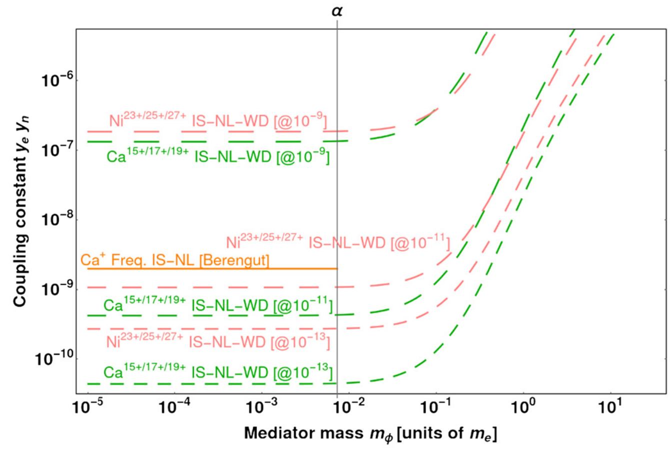

Fig. 3. Same as Fig. 2, with projected bounds from a King analysis of the weighted differences (IS-NL-WD: Isotope Shift-Nonlinearity with the Weighted Difference). The green curves refer to calcium [sparsely dashed (resp. dashed, densely dashed): projections on $^{40/42/44/48}Ca^{15+/17+/19+}$ assuming King planarity (KP) at the relative experimental accuracy of 10^{-9} (resp. 10^{-11}, 10^{-13})], the pink curves to nickel [sparsely dashed (resp. dashed, densely dashed): projections on $^{58/60/62/64}Ni^{23+/25+/27+}$ (KP at 10^{-9} (resp. 10^{-11}, 10^{-13}))].

the projected bounds appearing in pink in Fig. 2. For better experimental accuracies, King planarity breaks because of the subleading nuclear (SM) corrections, preventing the setting of bounds on NP in the present formalism. The peaks appearing on many curves in Fig. 2 arise from the cancellation of the term that appears as the factor of α_{NP} in Eq. (14) in a certain boson mass range, which corresponds to the cancellation of the denominator of the bound $\sigma_{\alpha_{\mathrm{NP}}}$.

We turn to deriving bounds from the $1s$ and $2p_{1/2}$ states (the respective ground states of the H-like and B-like ions) of the same four isotopes of calcium and nickel. It is expected [31] that pairs of electronic levels with more dissimilar wave functions can yield better tests, and indeed, we obtain a more stringent bound on the NP coupling constant with H-like/B-like pairs than with H-like/Li-like pairs, assuming a relative experimental accuracy of 10^{-11}. This is true for both calcium and nickel, as can be seen on Fig. 2.

Finally, the King analysis for isotope shifts can be combined with the weighted difference. We note that, just like the (leading) finite nuclear size correction to the g factor, the higher-order finite nuclear size correction, the nuclear deformation correction and the nuclear polarization correction scale as $1/n^3$ for ns states. The NP correction, however, scales as $1/n^2$ in the low carrier-mass limit [see Eq. (4b)], meaning that the $1s$–$2s$ weighted difference will also suppress the subleading nuclear corrections that cause King nonplanarities in the SM, while preserving the NP corrections. This makes the weighted difference a powerful tool to emphasise NP contributions to King nonplanarity. We repeat the same King analysis on the isotope shift with the pair of 'modified' g factors $\left[(g_1, g_2) = \left(\delta_{\xi_s} g, \delta_{\xi_p} g\right)\right]$ defined in Eq. (5). The corresponding bounds obtained from simulated data for calcium and nickel are given in Fig. 3. It is seen that use of the weighted difference is successful for calcium in particular: with the relative experimental accuracy of 10^{-13}, we find that King planarity would allow the setting of bounds on NP more than one order of magnitude more stringent than that obtained in Ref. [31]. Moreover, it appears that the interpretation of isotope shift data from experiments on singly charged ions is complicated by the SM contributions to King nonplanarity [69], which can, by contrast, straightforwardly be included in the formalism for few-electron highly charged ions, as discussed in detail in the present work. As mentioned above, there are plans [51] to measure differences of g-factors between two ions (1 and 2) with a relative precision $(g_1 - g_2)/g_1$ of up to 11 digits. In the case of calcium, and for the isotopes considered in the present work, the largest shift is the $^{40-48}Ca^{15+}$ isotope shift, which is roughly 1.6×10^{-6}. Hence, a measurement of this isotope shift with 11-digit precision would be equivalent to a measurement of the g factors with 17-digit precision, which is four orders of magnitude more precise than needed in our approach.

7. Conclusion and outlook

We have shown that g-factor measurements in highly charged ions provide a very competitive framework to obtain bounds on NP. Investigating the influence of a fifth force, acting between nucleons and electrons, on the g factor of bound electrons, we have used the isotope shift in g factors, and its combination with the weighted difference technique. We also accounted for subleading nuclear contributions to the isotope shift in the SM. The bounds readily obtained through existing data are between one and two orders of magnitude less stringent than those obtained [34] through published measurements of the isotope shift in transition frequencies in Ca^+. As we have found, measurement of isotope shifts in the g factor of H-like, Li-like and B-like calcium at the accuracy of 10^{-13}, projected to be easily achievable [51], can allow for the setting of bounds more than one order of magnitude more stringent than the ones obtained from the Ca^+ frequency shift. Isotope shifts in the g factor of bound electrons can also be used to obtain bounds on other hypothetical interactions [33], such as those arising in models with B–L vector bosons [70] or in chameleon models [71,72].

We thank Klaus Blaum for drawing our attention to the topic of Standard Model tests with atomic experiments, as well as Sven Sturm, Vladimir A. Yerokhin, Niklas Michel and Natalia S. Oreshkina for helpful conversations. This work is part of and supported by the German Research Foundation (DFG) Collaborative Research Centre "SFB 1225 (ISOQUANT)".

Declaration of competing interest

The authors declare that they have no known competing financial interests or personal relationships that could have appeared to influence the work reported in this paper.

Appendix A. Supplementary material

Supplementary material related to this article can be found online at https://doi.org/10.1016/j.physletb.2020.135527.

References

[1] T. Aoyama, M. Hayakawa, T. Kinoshita, M. Nio, Tenth-order QED contribution to the electron $g-2$ and an improved value of the fine structure constant, Phys. Rev. Lett. 109 (2012) 111807.
[2] D. Hanneke, S. Fogwell, G. Gabrielse, New measurement of the electron magnetic moment and the fine structure constant, Phys. Rev. Lett. 100 (2008) 120801.
[3] P.J. Mohr, D.B. Newell, B.N. Taylor, CODATA recommended values of the fundamental physical constants: 2014, Rev. Mod. Phys. 88 (2016) 035009.
[4] F. Jegerlehner, A. Nyffeler, The muon $g-2$, Phys. Rep. 477 (1) (2009).
[5] M. Lindner, M. Platscher, F.S. Queiroz, A call for new physics: the muon anomalous magnetic moment and lepton flavor violation, Phys. Rep. 731 (1) (2018).
[6] G.W. Bennett, et al., Measurement of the negative muon anomalous magnetic moment to 0.7 ppm, Phys. Rev. Lett. 92 (2004) 161802.
[7] G.W. Bennett, et al., Final report of the E821 muon anomalous magnetic moment measurement at BNL, Phys. Rev. D 73 (2006) 072003.
[8] W. Quint, J. Dilling, S. Djekic, H. Häffner, N. Hermanspahn, H.-J. Kluge, G. Marx, R. Moore, D. Rodriguez, J. Schönfelder, G. Sikler, T. Valenzuela, J. Verdú, C. Weber, G. Werth, HITRAP: a facility for experiments with trapped highly charged ions, Hyperfine Interact. 132 (2001) 457.
[9] S. Sturm, A. Wagner, B. Schabinger, J. Zatorski, Z. Harman, W. Quint, G. Werth, C.H. Keitel, K. Blaum, g factor of hydrogenlike $^{28}Si^{13+}$, Phys. Rev. Lett. 107 (2011) 023002.
[10] S. Sturm, A. Wagner, M. Kretzschmar, W. Quint, G. Werth, K. Blaum, g factor measurement of hydrogenlike $^{28}Si^{13+}$ as a challenge to QED calculations, Phys. Rev. A 87 (2013) 030501(R).
[11] S. Sturm, F. Köhler, J. Zatorski, A. Wagner, Z. Harman, G. Werth, W. Quint, C.H. Keitel, K. Blaum, High-precision measurement of the atomic mass of the electron, Nature 506 (7489) (2014) 467–470.
[12] S. Sturm, M. Vogel, F. Köhler-Langes, W. Quint, K. Blaum, G. Werth, High-precision measurements of the bound electron's magnetic moment, Atoms 5 (1) (2017).
[13] T. Beier, I. Lindgren, H. Persson, S. Salomonson, P. Sunnergren, H. Häffner, N. Hermanspahn, g_j factor of an electron bound in a hydrogenlike ion, Phys. Rev. A 62 (2000) 032510.
[14] V.A. Yerokhin, P. Indelicato, V.M. Shabaev, Evaluation of the self-energy correction to the g factor of s states in H-like ions, Phys. Rev. A 69 (2004) 052503.
[15] K. Pachucki, A. Czarnecki, U.D. Jentschura, V.A. Yerokhin, Complete two-loop correction to the bound-electron g factor, Phys. Rev. A 72 (2005) 022108.
[16] U.D. Jentschura, Binding two-loop vacuum-polarization corrections to the bound-electron g factor, Phys. Rev. A 79 (2009) 044501.
[17] V.A. Yerokhin, Z. Harman, Two-loop QED corrections with closed fermion loops for the bound-electron g factor, Phys. Rev. A 88 (2013) 042502.
[18] R.N. Lee, A.I. Milstein, I.S. Terekhov, S.G. Karshenboim, Virtual light-by-light scattering and the g factor of a bound electron, Phys. Rev. A 71 (2005) 052501.
[19] A. Czarnecki, R. Szafron, Light-by-light scattering in the Lamb shift and the bound electron g factor, Phys. Rev. A 94 (2016) 060501(R).
[20] A. Czarnecki, M. Dowling, J. Piclum, R. Szafron, Two-loop binding corrections to the electron gyromagnetic factor, Phys. Rev. Lett. 120 (2018) 043203.
[21] B. Sikora, V.A. Yerokhin, N.S. Oreshkina, H. Cakir, C.H. Keitel, Z. Harman, Theory of the two-loop self-energy correction to the g-factor in non-perturbative Coulomb fields, Phys. Rev. Res. 2 (2020) 012002(R).
[22] V.M. Shabaev, D.A. Glazov, G. Plunien, A.V. Volotka, Theory of bound-electron g factor in highly charged ions, J. Phys. Chem. Ref. Data 44 (3) (2015) 031205.
[23] P.J. Mohr, Self-energy radiative corrections in hydrogen-like systems, Ann. Phys. 88 (1974) 26.
[24] P.J. Mohr, G. Plunien, G. Soff, QED corrections in heavy atoms, Phys. Rep. 293 (1998) 227.
[25] V.M. Shabaev, Two-time Green's function method in quantum electrodynamics of high-Z few-electron atoms, Phys. Rep. 99 (2002) 69.
[26] V.A. Yerokhin, V.M. Shabaev, First-order self-energy correction in hydrogenlike systems, Phys. Rev. A 60 (1999) 800.
[27] V.M. Shabaev, D.A. Glazov, M.B. Shabaeva, V.A. Yerokhin, G. Plunien, G. Soff, g factor of high-Z lithiumilke ions, Phys. Rev. A 65 (2002) 062104.
[28] V.M. Shabaev, D.A. Glazov, N.S. Oreshkina, A.V. Volotka, G. Plunien, H.J. Kluge, W. Quint, g-factor of heavy ions: a new access to the fine structure constant, Phys. Rev. Lett. 96 (2006) 253002.
[29] V.A. Yerokhin, E. Berseneva, Z. Harman, I.I. Tupitsyn, C.H. Keitel, g factor of light ions for an improved determination of the fine-structure constant, Phys. Rev. Lett. 116 (2016) 100801.
[30] V.A. Yerokhin, E. Berseneva, Z. Harman, I.I. Tupitsyn, C.H. Keitel, Weighted difference of g factors of light Li-like and H-like ions for an improved determination of the fine-structure constant, Phys. Rev. A 94 (2016) 022502.
[31] J.C. Berengut, D. Budker, C. Delaunay, V.V. Flambaum, C. Frugiuele, E. Fuchs, C. Grojean, R. Harnik, R. Ozeri, G. Perez, Y. Soreq, Probing new long-range interactions by isotophe shift spectroscopy, Phys. Rev. Lett. 120 (2018) 091801.
[32] V.V. Flambaum, A.J. Geddes, A.V. Viatkina, Isotope shift, nonlinearity of King plots, and the search for new particles, Phys. Rev. A 97 (2018) 032510.
[33] C. Frugiuele, E. Fuchs, G. Perez, M. Schlaffer, Constraining new physics models with isotope shift spectroscopy, Phys. Rev. D 96 (2017) 015011.
[34] K. Mikami, M. Tanaka, Y. Yamamoto, Probing new intra-atomic force with isotope shifts, Eur. Phys. J. C 77 (2017) 896.
[35] P.W. Graham, D.E. Kaplan, S. Rajendran, Cosmological relaxation of the electroweak scale, Phys. Rev. Lett. 115 (2015) 221801.
[36] H.E. Haber, G.L. Kane, T. Sterling, The fermion mass scale and possible effects of higgs bosons on experimental observables, Nucl. Phys. B 161 (1979) 493.
[37] J. Jaeckel, S. Roy, Spectroscopy as a test of Coulomb's law: a probe of the hidden sector, Phys. Rev. D 82 (2010) 125020.
[38] V.M. Shabaev, Virial relations for the Dirac equation and their applications to calculations of hydrogen-like atoms, in: S.G. Karshenboim, V.B. Smirnov (Eds.), Precision Physics of Simple Atomic Systems, Springer-Verlag, 2003.
[39] J.A. Grifols, E. Massó, Constraints on finite-range baryonic and leptonic forces from stellar evolution, Phys. Lett. B 173 (1986) 237.
[40] G. Raffelt, Limits on a CP-violating scalar axion-nucleon interaction, Phys. Rev. D 86 (2012) 015001.
[41] J. Zatorski, B. Sikora, S.G. Karshenboim, S. Sturm, F. Köhler-Langes, K. Blaum, C.H. Keitel, Z. Harman, Extraction of the electron mass from g-factor measurements on light hydrogenlike ions, Phys. Rev. A 96 (2017) 012502.
[42] V.M. Shabaev, Finite nuclear size corrections to the energy levels of the multicharged ions, J. Phys. B, At. Mol. Opt. Phys. 26 (1993) 1103.
[43] D.A. Glazov, V.M. Shabaev, Finite nuclear size correction to the bound-electron g factor in a hydrogenlike atom, Phys. Lett. A 297 (2002) 408.
[44] V.A. Yerokhin, K. Pachucki, M. Puchalski, Z. Harman, C.H. Keitel, Electron-correlation effects in the g factor of light Li-like ions, Phys. Rev. A 95 (2017) 062511.
[45] M. Bordag, G.L. Klimchitskaya, U. Mohideen, V.M. Mostepanenko, Advances in the Casimir Effect, Oxford University Press, 2009.

[46] J. Redondo, G. Raffelt, Solar constraints on hidden photons re-visited, J. Cosmol. Astropart. Phys. 2013 (2013) 034.

[47] V.V. Nesvizhevsky, G. Pignol, K.V. Protasov, Neutron scattering and extra-short-range interactions, Phys. Rev. D 77 (2008) 034020.

[48] F. Köhler, et al., Isotope dependence of the Zeeman effect in lithium-like calcium, Nat. Commun. 7 (2016) 10246.

[49] W.H. King, Isotope Shifts in Atomic Spectra, Plenum Press, 1984.

[50] V.M. Shabaev, D.A. Glazov, A.V. Malyshev, I.I. Tupitsyn, Recoil effect on the g factor of Li-like ions, Phys. Rev. Lett. 119 (2017) 263001.

[51] S. Sturm, I. Arapoglou, A. Egl, M. Höcker, S. Kraemer, T. Sailer, B. Tu, A. Weigel, R. Wolf, J. Crespo López-Urrutia, K. Blaum, The ALPHATRAP experiment, Eur. Phys. J. Spec. Top. 227 (2019) 1425.

[52] V.A. Yerokhin, R.A. Müller, A. Surzhykov, P. Micke, P.O. Schmidt, Nonlinear isotope-shift effects in Be-like, B-like, and C-like argon, Phys. Rev. A 101 (2020) 012502.

[53] S.G. Karshenboim, V.G. Ivanov, Finite-nuclear-size contribution to the g factor of a bound electron: higher-order effects, Phys. Rev. A 97 (2018) 022506.

[54] A.V. Nefiodov, G. Plunien, G. Soff, Nuclear-polarization to the bound-electron g factor in heavy hydrogenlike ions, Phys. Rev. Lett. 89 (2002) 081802.

[55] A.V. Volotka, G. Plunien, Nuclear polarization study: new frontiers for tests of QED in heavy highly charged ions, Phys. Rev. Lett. 113 (2014) 023002.

[56] J. Zatorski, N.S. Oreshkina, C.H. Keitel, Z. Harman, Nuclear shape effect on the g factor of hydrogenlike ions, Phys. Rev. Lett. 108 (2012) 063005.

[57] N. Michel, J. Zatorski, N.S. Oreshkina, C.H. Keitel, Nonperturbative analysis of nuclear shape effects on the bound electron g factor, Phys. Rev. A 99 (2019) 012505.

[58] K. Pachucki, Nuclear mass correction to the magnetic interaction of atomic systems, Phys. Rev. A 78 (2008) 012504.

[59] G. Plunien, G. Soff, Nuclear-polarization contribution to the Lamb shift in actinide nuclei, Phys. Rev. A 51 (1996) 1119.

[60] G. Plunien, G. Soff, Erratum: Nuclear-polarization contribution to the Lamb shift in actinide nuclei, Phys. Rev. A 53 (1996) 4614.

[61] I. Angeli, K.P. Marinova, Table of experimental nuclear ground state charge radii: an update, At. Data Nucl. Data Tables 356 (2002) 119.

[62] P. Moller, J.R. Nix, W.D. Myers, W.J. Swiatecki, Nuclear ground-state masses and deformations, At. Data Nucl. Data Tables 59 (1995) 185.

[63] V.A. Yerokhin, C.H. Keitel, Z. Harman, Nuclear-size self-energy and vacuum-polarization corrections to the bound-electron g factor, J. Phys. B 46 (2013) 245002.

[64] V.M. Shabaev, V.A. Yerokhin, Recoil correction to the bound-electron g factor in H-like atoms to all orders in $Z\alpha$, Phys. Rev. Lett. 88 (2002) 091801.

[65] I.A. Aleksandrov, D.A. Glazov, A.V. Malyshev, V.M. Shabaev, I.I. Tupitsyn, Relativistic nuclear-recoil effect on the g factor of highly charged boronlike ions, Phys. Rev. A 98 (2018) 062521.

[66] R.X. Schüssler, et al., Recent developments at the high-precision mass spectrometer PENTATRAP, AIP Conf. Proc. 18 (2016) 011020.

[67] A. Rischka, H. Cakir, M. Door, P. Filianin, Z. Harman, W.J. Huang, P. Indelicato, C.H. Keitel, C.M. König, K. Kromer, M. Müller, Y.N. Novikov, R.X. Schüssler, Ch. Schweiger, S. Eliseev, K. Blaum, Mass-difference measurements on heavy nuclides with an eV/c^2 accuracy in the PENTATRAP spectrometer, Phys. Rev. Lett. 124 (2020) 113001.

[68] R.X. Schüssler, H. Bekker, M. Braß, H. Cakir, J.R. Crespo López-Urrutia, M. Door, P. Filianin, Z. Harman, M.W. Haverkort, W.J. Huang, P. Indelicato, C.H. Keitel, C.M. König, K. Kromer, M. Müller, Y.N. Novikov, A. Rischka, Ch. Schweiger, S. Sturm, S. Ulmer, S. Eliseev, K. Blaum, Detection of metastable electronic states by Penning trap mass spectrometry, Nature 581 (7806) (2020) 42.

[69] I. Counts, J. Hur, D.P.L. Aude Craik, H. Jeon, C. Leung, J.C. Berengut, A. Geddes, A. Kawasaki, W. Jhe, V. Vuletić, Observation of 3σ nonlinear isotope shift in Yb^+ search for new boson, arXiv:2004.11383, 2020.

[70] D. Feldman, P.F. Perez, P. Nath, R-parity conservation via the Stueckelberg mechanism: LHC and dark matter signals, J. High Energy Phys. 2012 (2012) 38.

[71] J. Khoury, A. Weltman, Chameleon fields: awaiting surprises for tests of gravity in space, Phys. Rev. Lett. 93 (2004) 171104.

[72] J. Khoury, A. Weltman, Chameleon cosmology, Phys. Rev. D 69 (2004) 044026.